Prospects of EM follow-up of NSBH mergers in the LIGO-India era

Yogita Kumari
Inter-University Centre for Astronomy and Astrophysics, Pune

July 18, 2025

Abstract

Gravitational wave(GW) physics is a new tool to probe the universe. Compact Binary Coalescences (CBCs) are one of the sources of GWs. If there is a possibility of getting EM follow-up of a few tens of CBCs, involving neutron stars, the Hubble tension may get resolved. This project is about exploring the possibility of getting EM follow-up of NSBH mergers with 3 LIGO detectors (Livingston, Hanford, and India). A neutron Star Blackhole (NSBH) merger can have an electromagnetic counterpart based on its mass and spin. Since they are relatively massive than Binary Neutron Star(BNS) Mergers, they can be detected at relatively higher redshifts, so there is a possibility of getting the Hubble parameter as well. First, the sensitivity of LIGO detectors for NSBH mergers is determined. Second, with BAYESian TriAngulation and Rapid localization(Bayestar), these events are localized in the sky for EM follow-up. Lastly, an estimation of the time required for EM follow-up using the Legacy Survey of Space and Time(LSST) is done. It is found that there is a plausibility of getting EM follow-up of NSBH mergers based on the results of these steps.

1 Introduction

1.1 Physics of Gravitational waves

GWs are generated by accelerating masses. In this section, a brief introduction to the physics of the propagation, effect, and generation of Gravitational waves(GWs) is provided [1]. $G = 1$ and $c = 1$ are taken. Greek letters denote spacetime coordinates$(0, 1, 2, 3)$ and Latin letters denote spatial coordinates $(1, 2, 3)$.

1.1.1 Propagation of Gravitational waves

In order to understand how GWs propagate through spacetime, take the weak gravitational field limit. In this limit, spacetime can be considered nearly flat (far from a changing gravitational source, such that the effect of this source has already reached that point). At this point, one can choose a coordinate system in which the metric is given by

$$g_{\mu\nu} = \eta_{\mu\nu} + h_{\mu\nu} \tag{1}$$

such that $|h_{\mu\nu}| << 1$. $h_{\mu\nu}$ remains invariant under Lorentz transformation so one can assume $h_{\mu\nu}$ as an tensor in SR. It also remains invariant under Gauge transformation ($x^\mu \rightarrow x^\mu + \xi^\mu$

where $|\xi^{\mu}{}_{,\nu}| << 1$).
Using these properties, one can construct a coordinate system known as the Lorentz frame in which the Einstein equation becomes

$$\Box \bar{h}_{\mu\nu} = -16\pi T_{\mu\nu} \tag{2}$$

Far from the source,

$$\Box \bar{h}_{\mu\nu} = 0$$

This gives a wavelike solution with propagation speed c, which is given by

$$\bar{h}_{\mu\nu} = \int \frac{d^3k}{(2\pi)^3} \mathrm{Re}(A_{\mu\nu}(\mathbf{k}) e^{\iota k_p x^p}) \tag{3}$$

where, $\bar{h}^{\mu\nu} = h^{\mu\nu} - \frac{1}{2}h$ is trace reverse of $h_{\mu\nu}$.
If one further goes to the transverse traceless gauge. Assuming GW is propagating in the z direction.

$$A^{(\mathrm{TT})}_{\mu\nu} = \begin{pmatrix} 0 & 0 & 0 & 0 \\ 0 & A^{(\mathrm{TT})}_{xx} & A^{(\mathrm{TT})}_{xy} & 0 \\ 0 & A^{(\mathrm{TT})}_{xy} & -A^{(\mathrm{TT})}_{xx} & 0 \\ 0 & 0 & 0 & 0 \end{pmatrix} \tag{4}$$

1.1.2 Effect of GW

Consider a particle at rest before it encounters GW.($u^i = 0$). If one chooses Lorentz frame and TT gauge in that, then the geodesic equation at initial time t_0 is given by

$$\left(\frac{du^\mu}{d\tau} + \Gamma^\mu_{\nu\delta} u^\nu u^\delta \right)\Big|_{t_0} = 0 \tag{5}$$

$$\left.\frac{du^\mu}{d\tau}\right|_{t_0} = -\left.\Gamma^\mu_{00}\right|_{t_0} = 0 \tag{6}$$

$$\tag{7}$$

This implies that at the initial time, acceleration is zero, which means that 4-velocity u^μ remains the same after some time $t_0 + \delta t$. So, again, since 4-velocity u^μ is $(1, 0, 0, 0)$, the same results, so a particle initially at rest is going to stay at rest (no change in coordinates of two particles). In order to see the effect of GW, consider two nearby particles at an instant of time (let as t) at positions $(0, 0, 0)$ and $(0, 0, \epsilon)$ respectively, so the proper distance between them will be

$$\delta l = \int \sqrt{|ds^2|} \approx \epsilon \left(1 + \frac{1}{2} h_{xx}(t, \mathbf{0}) \right) \tag{8}$$

The proper distance is going to change due to GW.
Instead of the TT gauge, if one tries to evaluate the change in the Local Inertial Frame(LIF), then the connecting vector ξ^μ starting from one particle (in LIF) to another changes as

$$\partial_t^2 \xi^x = \frac{1}{2} \partial_t^2 h^{TT}_{xx} \xi^x + \frac{1}{2} \partial_t^2 h^{TT}_{xy} \xi^y \tag{9}$$

$$\partial_t^2 \xi^y = \frac{1}{2} \partial_t^2 h^{TT}_{xy} \xi^x - \frac{1}{2} \partial_t^2 h^{TT}_{xx} \xi^y \tag{10}$$

$$\partial_t^2 \xi^z = 0 \tag{11}$$

This can be interpreted as if, from the perspective of a particle whose LIF is taken, there is a tidal force acting on another particle.

1.1.3 Generation of Gravitational waves

In order to find $h_{\mu\nu}$ due to the presence of the energy momentum tensor $T_{\mu\nu}$, we need to use eq (2). This equation is solved using the Green function.

$$\Box G(x^\mu, x^{\mu'}) = \delta^4(x^\mu - x^{\mu'})$$
$$G(x^\mu, x^{\mu'}) = \frac{1}{4\pi}\frac{\delta(t-(t'-|\mathbf{r}-\mathbf{r}'|))}{|\mathbf{r}-\mathbf{r}'|}$$
$$\bar{h}_{\mu\nu} = \int dt' \int d^3x' G(x^\mu, x^{\mu'})(-16\pi T_{\mu\nu})$$

When one tries to calculate gravitational strain h_{ij} far from the source in the TT gauge with the use of local conservation of the energy-momentum tensor,

$$h_{ij} = \frac{2}{d_L}\frac{d^2Q_{ij}}{dt^2} \tag{12}$$

where $Q_{ij} = \int d^3x \rho(\mathbf{x}) \left(x_i x_j - \frac{1}{3}r^2\delta_{ij}\right)$ is a quadrupole moment.

Energy carried by GWs is given by

$$\frac{dE_{GW}}{dt} = \frac{1}{5}\sum_{i,j=1}^{3}\frac{d^3Q_{ij}}{dt^3}\frac{d^3Q_{ij}}{dt^3} \tag{13}$$

1.2 GW from CBCs

In this section, I tried to give a physically intuitive idea based on [2] about GW emission from CBCs. GW emission from a binary system can be described by three phases: Inspiral, Merger, and Ringdown. In the inspiral phase, the motion of the two components (compact objects, blackhole, neutron star) of the binary system leads to GW emission. Due to the GW emission, components start to come closer. In the early inspiral phase, orbits of components of a binary system can be approximated as circles; this is known as the quasi-circular approximation As orbits come closer, frequency increases, and GW emission increases (Amplitude increases). This approximation can be applied till Innermost Stable Circular Orbit (ISCO). After it, there is going to be a plunge-in phase in which orbits will be essentially non-circular and components will plunge inwards. After that, the components go through a merger, ending up as a blackhole or a neutron star. This end object oscillates and comes to equilibrium at some frequency. This phase is known as Ringdown.

1.2.1 IMRPhenomD

In order to find whether there is a GW source present in the GW data from a ground-based detector or not, one tries to find a particular kind of waveform in the data (Explained in detail in 1.3). There are models to get these waveforms. IMRPhenomD is a frequency domain phenomenological model of the GW emission signal from a binary black hole for Inspiral, Merger, and Ringdown [3]. It can be used to get a waveform for mass ratio $q = 1:18$

and dimensionless spin parameter $a/m \sim 0.85$ (for equal masses 0.98). The inspiral phase is described by the Effective One-Body (EOB) approximation. Merger-Ringdown are modelled with Numerical Relativity (NR). Different parts of the model are connected by demanding continuity in the phase and amplitude of the wave.

1.3 Analysis of GW data

This section is about determining whether the GW signal is present or not in the GW detector output, and if present, what is the source (for further details [4]). For ground-based interferometry detectors (LIGO detectors), we get strain data. This data contains not only the signal (may or may not) but also noise from the detector.

1.3.1 PSD

Incoming GW radiation leads to a phase shift in light, which combines after moving through the interferometer's two arms. This produces a scalar quantity strain, which is related to the incoming tensor quantity by $h = D^{ij}h_{ij}$. Here, D^{ij} is the detector tensor. The output of the detector, which is observed, is this signal + noise $s(t) = h(t) + n(t)$. If the detector is a linear system, then the output, in frequency space, of an input signal $h(t)$ is

$$\tilde{h}_{\text{out}}(f) = T(f)\tilde{h}(f) \tag{14}$$

Here, $T(f)$ is the transfer function.
Noise from the detector is added at multiple stages. So, the transfer function is $T(f) = \prod_i T_i(f)$, where i indicate i^{th} stage of detector. Let's say the total noise at output is $n_{\text{out}}(f)$. Instead of considering noise at each stage, one can consider a fictitious noise at the input of the detector, which is transferred by $T(f)$.
$\tilde{n}(f) = T^{-1}\tilde{n}_{\text{out}}(f)$.
If one considers the noise to be stationary, then its Fourier components are going to be independent of each other. Noise Power Spectral Density (PSD) is defined as

$$S_n(f) = \lim_{T \to \infty} \frac{2}{T} \left| \int_{-\frac{T}{2}}^{\frac{T}{2}} dt\ n(t) e^{-2\pi \iota f t} \right|^2$$

It is calculated using the Welch method [5].

1.3.2 Detector Pattern Function

The detector's sensitivity is different in different directions. If the source is face on (h_+ and $h_\times$ are defined in a plane which is perpendicular to GW propagation), the observed strain is given by

$$h(t) = h_+(t)F_+(\theta, \phi) + h_\times(t)F_\times(\theta, \phi) \tag{15}$$

where F_+ and $F_\times$ are detector pattern functions. This $h(t)$ does not depend on polarization angle ψ.

1.3.3 Match Filtering and SNR

The GW signal is buried inside the noise of larger amplitude, so in order to extract the signal, we need to know the form of the signal to some extent. In order to know the highest possible Single to Noise Ratio (SNR), a filter function $K(t)$ is defined

$$\hat{s} = \int_{-\infty}^{\infty} dt\ s(t)\ K(t) \tag{16}$$

SNR ρ is defined as ratio of expected of value of $\hat{s}$ (S) and rms value of $\hat{s}$ in absence of signal (N)

$$\rho = \frac{S}{N} = \frac{(u|h)}{(u|u)^{1/2}} \tag{17}$$

where inner product is defined as$(A, B) = 4\ \mathrm{Re} \int_0^\infty \frac{\tilde{A}^*(f)\tilde{B}(f)}{S_n(f)}$ and $\tilde{u}(f) = \frac{1}{2} S_n(f)\tilde{K}(f)$. To get the maximum value of ρ, $\tilde{u}(f)$ need to be proportional to $\tilde{h}(f)$

$$\tilde{K}(f) = \mathrm{const} \frac{\tilde{h}(f)}{S_n(f)}$$

This is known as the Wiener filter.
So,**Optimal SNR** is given by

$$\rho = (h|h)^{1/2} \tag{18}$$

1.4 Definitions related to distance measurements

Some important definitions related to distance are given in this section, as mentioned in [6].

1.4.1 Horizon Distance(d_h)

It is a luminosity distance beyond which SNR goes below the SNR threshold at the optimal sky location and binary inclination.

1.4.2 Sensitivity Volume

Horizon distance is the farthest one can see, but at different locations and inclinations, it could vary, so the sensitive volume in which detection can be made is different from the horizon distance volume $V_h = \frac{4}{3}\pi d_h^3$. This is obtained via averaging over the antenna pattern, binary inclinations, and orientations.

1.5 Concept of Sky localization

GW detectors are not unidirectional, so just detection could not tell at what sky position the source is. For EM telescopes to follow, there is a need to identify the sky position. To determine position in the sky, more than one detector is required.

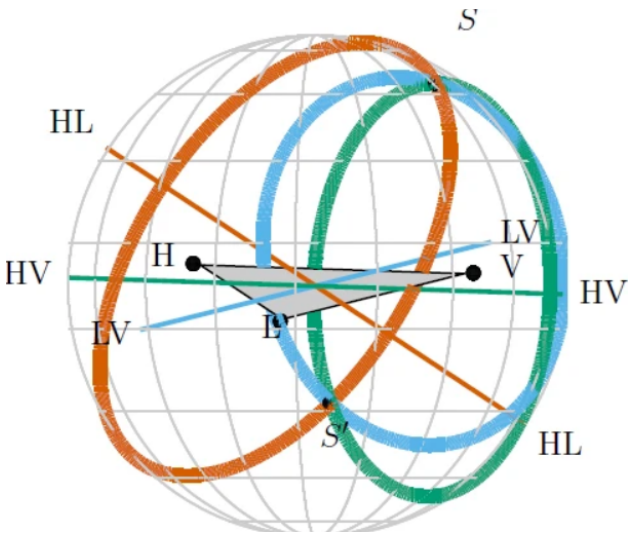

Figure 1: Triangularization with two LIGO detectors (Livingston and Hanford) and the Virgo detector. Credit:[7]

1.5.1 Triangularization

The basic idea of Triangularization is to localize the source by measuring the time delay of arrival of the signal. If two detectors happen to detect an event. They can give a circle of points with the same time delay in the sky at which the event could be situated. Due to time uncertainty, this circle will have a width, i.e., there will be an annulus. Since the GW detector is not equally sensitive in all directions, this information can be further used to localize the source better. If three detectors happen to detect the event, then one gets 2 points opposite to each other with some width due to detector time uncertainty, projected on the plane of the three detectors as shown in Figure:1.
Time uncertainty for CBC is given by $\sigma_t \approx (2\pi\rho\sigma_f)^{-1}$ where ρ is SNR, σ_f is the effective bandwidth of the signal in the detector. This time uncertainty gives sky localization accuracy as discussed in [8]. Here is an overview of sky localization with two detectors as given in present in [8].
Two-site network:
Let there be a source on a unit sphere at $\mathbf{R}$ position. Two detectors are separated by $\mathbf{D}$, so the arrival time difference between the two sites is $T_1 - T_2 = \mathbf{D}.\mathbf{R}$.
Taking timing accuracies σ_1 and σ_2 for the two detectors, the distribution of time observed is given by

$$p(t_1, t_2|s) \propto p(t_1, t_2) \exp\left[-\frac{(t_1 - T_1)^2}{2\sigma_1^2} - \frac{(t_2 - T_2)^2}{2\sigma_2^2}\right] \tag{19}$$

The measured time delay is $t_1 - t_2$. Using this time delay, position is determined, let's say it is $\mathbf{r}$, so if the distribution is marginalised over arrival time and taking a uniform prior, the distribution of observed time delay

$$p(\mathbf{r}|\mathbf{R}) \propto p(\mathbf{r}) \exp\left[-\frac{(\mathbf{D}.(\mathbf{r} - \mathbf{R}))^2}{2(\sigma_1^2 + \sigma_2^2)}\right] \tag{20}$$

This suggests that sky localization will be better given that time uncertainties are smaller and the baseline is longer.
Other than time uncertainty, systematic errors due to uncertainty in waveform and calibration of the instruments can also affect the sky localization.

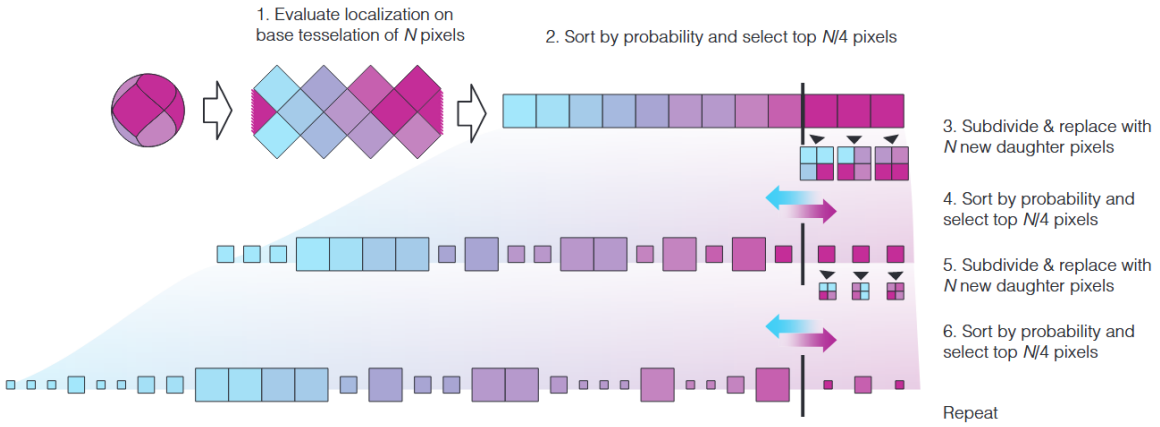

Figure 2: HEALPix sampling in BAYESTAR. Credit:[10]

1.5.2 Molleweide Projection

It is an equal area pseudocylindrical projection of a sphere. This is used to project the values of a spherical surface onto a plane.

1.5.3 Hierarchical Equal Area isoLatitude Pixelation of a sphere(HEALPix)

It is pixelization of the sky in a way that angular resolution can be increased. It starts with dividing the sky into 12 equal areas tiles. Now, at successive orders, each tile is divided into 4 tiles [9].

1.5.4 Bayestar

Sky localization of the GW source needs to be done faster so that EM telescopes can follow it. BAYESian TriAngulation and Rapid localization(BAYESTAR) is a tool used for rapid sky localization without any need for full parameter estimation [10]. It is based on the assumption that the matched-filter values of amplitude, phase, and time are enough to give information about sky localization. Intrinsic parameters are taken to be equal to their maximum likelihood estimate.
The marginalized posterior probability is calculated at the center of HEALPix pixels (3072). These pixels are ranked in descending order of posterior probability. Take one-fourth of the original number of pixels (daughter pixels) and subdivide them into the original number of pixels. Calculate again the posterior at the center of the daughter pixels. Again, subdivide into daughter pixels, sort in descending order, and do this 7 times (Figure:2). For each pixel, the posterior probability can be calculated independently, so parallelization can be done.
In order to calculate the area, HEALPix pixels were sorted in descending posterior probability. When the total value reaches 0.9, then the pixel index multiplied by the area per pixel is called 90% credible area.
The searched area is defined as the smallest area containing the true location of the source.

1.6 Electromagnetic Counterpart for NSBH mergers

The NSBH merger can have an EM counterpart as well, given that the tidal radius (the Roch limit) is larger than ISCO [11]. Whether or not a neutron star will get tidal disrupted depends on the mass ratio, the spin of the blackhole, and the neutron star's equation of

state [12].
Here, I tried to present an order of magnitude calculation for the maximum mass of a blackhole possible based on simple arguments given in [13] and [14]. To calculate the Roche limit, imagine a blackhole and a neutron star of mass density ρ_M and ρ_m, and radius R and r, respectively. They are d distance apart (center-to-center distance). The NS rotates around the BH with angular speed ω. Now, we take an infinitesimal point of mass dm of the NS closest to the BH. If one assumes that rotation is synchronous, this point will move on a circular path around BH. To disintegrate, forces acting outward on NS must be greater than forces holding it. Three forces act in the rest of this point.
(i) Gravitational force due to the BH

$$F_1 = \frac{GMdm}{(d-r)^2}$$

where $M = \rho_M(\frac{4}{3}\pi R^3)$
(ii) Self-gravity of NS

$$F_2 = \frac{Gmdm}{r^2}$$

where $m = \rho_m(\frac{4}{3}\pi r^3)$
(ii) Centrifugal force due to the rotating frame

$$F_c = dm\omega^2(d-r)$$

ω can be calculated using $\omega^2 d = \frac{GM}{d^2}$

$$\begin{aligned} F_c =& dm\frac{GM}{d^3}(d-r) \\ =& \frac{GMdm}{d^2} - \frac{GMdmr}{d^3} \end{aligned}$$

When all three forces are in equilibrium

$$\begin{aligned} \frac{GMdm}{(r_R-r)^2} =& \frac{Gmdm}{r^2} + \frac{GMdm}{r_R^2} - \frac{GMdmr}{r_R^3} \\ \frac{1}{(r_R-r)^2} =& \frac{1}{r^2}\frac{m}{M} + \frac{1}{r_R^2} - \frac{r}{r_R^3} \\ \frac{1}{r_R^2}\frac{1}{(1-\frac{r}{r_R})^2} =& \frac{1}{r^2}\frac{m}{M} + \frac{1}{r_R^2} - \frac{r}{r_R^3} \end{aligned}$$

Now $r << r_R$

$$\begin{aligned} \frac{1}{r_R^2}\left(1+2\frac{r}{r_R}\right) =& \frac{1}{r^2}\frac{m}{M} + \frac{1}{r_R^2} - \frac{r}{r_R^3} \\ 3\frac{r}{r_R^3} =& \frac{1}{r^2}\frac{m}{M} \\ r_R^3 =& 3r^3\frac{M}{m} \\ r_R^3 =& 3r^3\frac{\rho_M(\frac{4}{3}\pi R^3)}{\rho_m(\frac{4}{3}\pi r^3)} \\ r_R =& 1.44\left(\frac{\rho_M}{\rho_m}\right)^{\frac{1}{3}} R \end{aligned}$$

This is the Roche limit for two solid bodies. In the case of fluid bodies, there are corrections required since the spherical assumption no longer holds, and the Roche limit will be

$$r_R = 2.4 \left(\frac{\rho_M}{\rho_m} \right)^{\frac{1}{3}} R$$

For tidal disruption $r_R \geq R_{ISCO}$. Taking the BH mass M_{BH}, the NS density ρ

$$\begin{aligned} r_R &\geq R_{ISCO} \\ 2.4 \left(\frac{\rho_{M_{BH}}}{\rho} \right)^{\frac{1}{3}} R_s &\geq R_{ISCO} \\ 2.4 \left(\frac{\frac{M_{BH}}{\frac{4}{3}\pi R_s^3}}{\rho} \right)^{\frac{1}{3}} R_{ISCO} &\geq R_{ISCO} \\ 2.4 \left(\frac{M_{BH}}{\frac{4}{3}\pi R_{ISCO}^3 \rho} \right)^{\frac{1}{3}} &\geq 1 \end{aligned}$$

Now,ISCO for non spinning BH $R_{ISCO} = \frac{6GM_{BH}}{c^2}$

$$\begin{aligned} 2.4 \left(\frac{M_{BH}}{\frac{4}{3}\pi \left(\frac{6GM_{BH}}{c^2} \right)^3 \rho} \right)^{\frac{1}{3}} &\geq 1 \\ M_{BH}^{\frac{2}{3}} \leq 2.4 \left(\frac{1}{\frac{4}{3}\pi \left(\frac{6G}{c^2} \right)^3 \rho} \right)^{\frac{1}{3}} \\ M_{BH} \leq 2.4^{\frac{3}{2}} \left(\frac{1}{\frac{4}{3}\pi \left(\frac{6G}{c^2} \right)^3 \rho} \right)^{\frac{1}{2}} \\ M_{BH} \leq 0.12 \left(\frac{c^6}{G^3 \rho} \right)^{\frac{1}{2}} \end{aligned}$$

for a typical neutron star density $\rho = 3.7 \times 10^{17}$ kg m^{-3} [15], $M_{BH} \leq 5 M_\odot$

When the neutron star is tidally disrupted equatorially, an accretion disk will form, and some matter will be ejected. Accreting matter can lead to the formation of a jet, and short gamma-ray bursts (sGRBs) can be observed. Ejected neutron-rich material will undergo the r-process, and heavy nuclei will form through neutron capture. These heavy nuclei will eventually go through radioactive decay. This will lead to neutrino emission and γ rays emission in the initial few hours, and then emission in the ultraviolet, optical, and infrared range (UVOIR). This is known as a kilonova. It lasts for a few days.

2 NSBH Merger Detection Methodology

2.1 Sensitivity of GW detector

To know about the possibility of NSBH detection with the LIGO network (LHI- Livingston, Hanford, India), two key points to understand are: (i) till what distance we can detect NSBH merger and for what mass (Horizon distance for a particular mass), (ii) for what distance we are going to get maximum detection.

2.1.1 Horizon distance

The distance beyond which the network SNR threshold falls below 12[16] for an optimally oriented binary (face on to the detector), is called the horizon distance. Any source that is within this distance has some probability of being detected. To calculate this distance for NSBH mergers, the following steps are taken.

1. Blackhole mass is taken in the range $3-10M_{\odot}$ since low mass blackhole are more likely to give EM counterparts[17]. For the neutron star, two mass values were taken $1.4M_{\odot}$ and $2M_{\odot}$. As mentioned in [18], the mass distribution of galactic double neutron stars is given by a Gaussian distribution with mean value $1.33M_{\odot}$ and width $0.09M_{\odot}$. So, a single value is taken since the horizon distance won't change much due to the mass of the neutron star. Two different values are taken so that we can compare whether or not there is a difference in horizon distance.

2. The NSBH system is assumed to be face-on, which implies that the polarization angle won't impact the amplitude received.

3. The Model of the universe is taken as ΛCDM with 0.3 fraction of energy density as matter and the remaining 0.7 as dark energy.

4. Three LIGO detectors (**LHI- Livingston, Hanford, India**) are taken to observe the merger. The noise PSD for these detectors is taken as A+.

5. IMRPhenomD waveform family is used to generate the signal.

6. In order to take into account differential directional sensitivity (antenna pattern) in different directions, 48 uniformly selected random RA, DEC are taken.

7. **Optimal SNR** (18) is calculated by taking the square root of the inner product of the signal with itself at a particular time for all directions.

8. For a particular primary mass, SNR is calculated at all redshifts. For a particular redshift value, SNR is calculated for all 48 directions [19](If we place the same source in different directions). Now, it is checked whether the SNR is below 12 or not. If at a redshift (let's say z_1), SNR just goes below 12(let's say ρ_1), then we calculate the redshift at which SNR becomes 12 by linear interpolation between the point just before SNR becomes below 12 (z_0, ρ_0) and z_1. Redshift at SNR=12 is given by

$$z = \frac{z_1 - z_0}{\rho_1 - \rho_0}(12 - \rho_0) + z_0$$

9. The value of z for all 48 directions is calculated. Then, sort the value of z in increasing order. The highest redshift is going to give the horizon. These sources are distributed

at different redshifts. 50% of these sources could be detected from the horizon to the distance (or redshift) at which they have an SNR value of 12. To get this redshift, we took the redshift at which 24 sources or directions are giving an SNR value above 12. For 90%, we took the value for which 90% of the directions have an SNR value above 12. If there is a source of a particular mass at redshift of 50%, then there are 50% chances that it could be detected. For 90% redshift, there are 90% chances that it could be detected.

10. For each mass, calculations from the above two steps are made.

11. At last, A spline fit is done to get a smoother version.

2.1.2 Distance with maximum detection possibility

As one goes to greater distances, SNR goes down, but the number of mergers increases as well since volume is increasing as the distance squared. In order to find the distance at which different mergers can be detected, the following steps are taken.

1. Same kind of mass distribution, sky distribution, position in sky, model of signal, is taken as in Horizon distance calculations. NS mass is taken as $1.4M_{\odot}$.

2. For all directions, redshifts are calculated at which the SNR is 12 for each mass.

3. At a particular redshift, if there are some directions at which SNR is 12 or below, then the source could not be detected in those directions, which suggests that detecting a source at that redshift has a probability based on its position on the sky. As one goes farther from the source, the probability of detection decreases.
   To find how this probability changes as a function of redshift for a particular mass, redshifts found in the step before are arranged in increasing order and stored in an array z_h. Probability of detection is taken to be 1 at the smallest redshift in z_h and below; and 0 at the highest redshift in z_h and above. 999 points are taken in between them. Redshift is increased and probability is taken to be 1 until the point, the next point in z_h is crossed. Once redshift becomes greater than the next value from z_h, the probability decreases by a factor of $\frac{1}{\text{length of } z_h}$. Again, redshift is increased until the next point in z_h is crossed. This goes on till the last point of the array. We get a kind of step function, starting from 1 to zero, dropping by a factor of $\frac{1}{\text{length of } z_h}$. This is fitted with a polynomial of order 5. This way, we get the Probability of detection as a function of redshift and mass $F(m, z)$.

4. For a particular redshift, this $F(m, z)$ is summed over all masses to give the total probability at a particular redshift $P(z)$.

5. If one assumes a uniform number density of NSBH mergers in a shell as one goes higher and higher distance, the number of detections(N_D) is proportional to $d_L^2 \times P(z)$.

6. For distances 100 Mpc to 2500 Mpc, the number of detections N_D is calculated and normalized by the total detections in the 100-2500 Mpc range.

2.2 Sky Localization

GW detectors are not unidirectional, so upon a detection, it is hard to tell in which direction the source is. On the other hand, EM telescopes are directional, so for EM follow-up of GW

detection, there is a need for the localization of the source. This can be done with the triangulation of the source with 2 or more detectors.
The task of sky localization is performed using Bayestar[10].

1. PSDs for all detectors are generated using as aLIGOAPlusDesignSensitivityT1800042.

2. Bayestar injection tool is used to generate stimulated NSBH sources with mass distribution same as in section:3 and spin zero. First, this tool divides the parameter space (masses and spins) into $10 \times 10 \times 10 \times 10$ grid. There are going to be 10^4 4D boxes. For a particular box horizon distance is calculated for all sources in that box. This gives an idea about what the distance cutoff is beyond which sources with those parameters will have an SNR below the SNR threshold. Now this information is further used to put sources in a uniform and spatially isotropic sensitive volume so that fewer computational resources are used. A total of 1000 injections are created from randomly uniform 1000 BH masses in the range 3 to 10 $M_\odot$ with SNR 8 in a single detector and a minimum trigger in 2 detectors.

3. Bayestar_realize_coincs tool is used to figure out which of the given stimulated sources from the Bayestar injection are going to be identified as triggers. SNR is calculated using a matched-filtering search pipeline. Gaussian measurement error is introduced in the SNR time series. Injections that are detected in coincidence in more than one detector with SNR greater than the threshold SNR 12 are called coincidence events. Total 89 events are found as coincidences.

4. Bayestar_localize_coinc is used for localizing the coincidence sources and generating fits files.

5. Using ligo-skymap-stats, the searched area for all coincidence events is found. Median, mean, minimum, and maximum searched area (section:1.5.4) are found using these results.

2.3 EM follow up

The LSST telescope can be used for kilonova follow-up. In order to figure out how much exposure time is required for LSST observation, one needs to figure out how much time is required. For constant SNR (from [20]), Exposure time t and photon rate are inversely proportional to each other. Photon rate is proportional to flux F. Flux is proportional to $10^{-0.4m}$ where m is the apparent magnitude of the source. Distance (d) and apparent magnitude are related by

$$m - M = 5 \log \left(\frac{d}{pc} \right) - 5$$

where M is the absolute magnitude.
This implies that

$$t \propto 10^{0.4m}$$
$$t = \text{Const} 10^{0.4m}$$
$$t = \text{Const } 10^{0.4\left(M+5\log\left(\frac{d}{pc}\right)-5\right)}$$

For LSST, it takes 30 seconds for a 24.52 magnitude source in i-band [21]. so Const $= 30 \times 10^{-0.4\times 24.52}$

$$t = 30 \times 10^{-0.4\times 24.52} 10^{0.4\left(M+5\log\left(\frac{d}{pc}\right)-5\right)} \text{ sec}$$

For a kilonova, taking the typical value of absolute value in the r-band is -13 (taken from [10])

$$\begin{aligned} t &= 30 \times 10^{0.4\left(-13+5\log\left(\frac{d}{pc}\right)-5-24.52\right)} \text{ sec} \\ &= 30 \times 10^{0.4\left(5\log\left(\frac{d}{pc}\right)-42.52\right)} \text{ sec} \\ &= 30 \times 10^{2\log\left(\frac{d}{pc}\right)} \times 10^{-17.008} \text{ sec} \\ &= 2.94 \times 10^{-16} \times \left(\frac{d}{pc}\right)^2 \text{ sec} \end{aligned}$$

This is the exposure time required for a kilonova at luminosity distance d.

3 Results

The results are as follows:

- Horizon distance plots for NSBH mergers with neutron star mass $M_{NS} = 1.4M_\odot$ and $M_{NS} = 2M_\odot$ are shown in Figure:3. One can see there is not much difference in the horizon distance value, so taking a single value is justified.

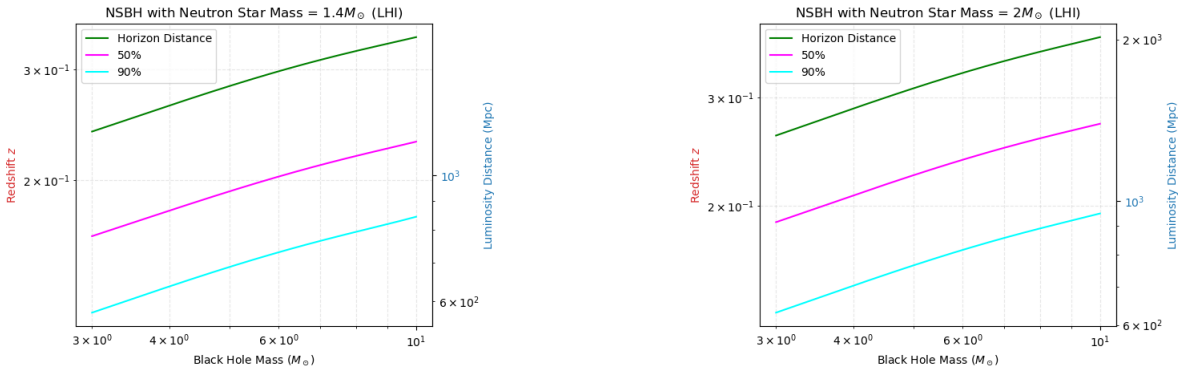

(a) $M_{NS} = 1.4M_\odot$ (b) $M_{NS} = 2M_\odot$

Figure 3: Sensitivity of LIGO detectors for NSBH mergers. Here, the horizon distance tells about the distance beyond which there is no possibility of detection. 50% line tells about the distance at which there is 50% chance of getting detected. 90% line tells about the distance at which there is 90% chance of getting detected.

- Plot of fraction of NSBH mergers detected at different redshifts is as shown in Figure:4. The maximum number of NSBH detections can be made at redshift $z \approx 0.23$. This corresponds to a luminosity distance of 1161.14 Mpc. It is found that till this distance, almost 50% of all detections are there, starting from 100 Mpc distance.
- Sky localization of 1000 NSBH sources using Bayestar gave median, mean, minimum, and maximum searched areas as 3.69, 28.75, 0.00, and 554.14 square degrees. (See Figure:5).

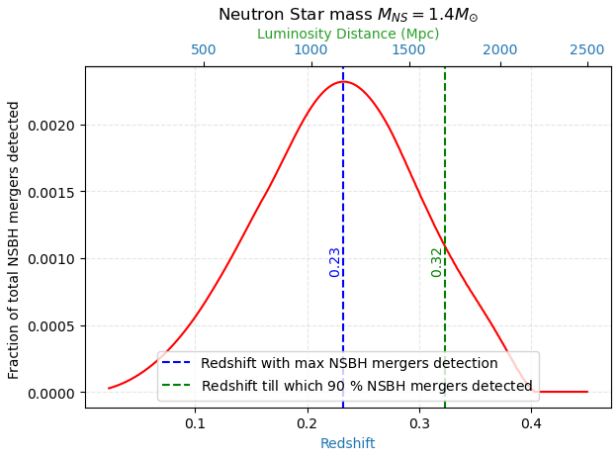

Figure 4: Fraction of total NSBH mergers (in $100-2500$ Mpc) detected at different distances

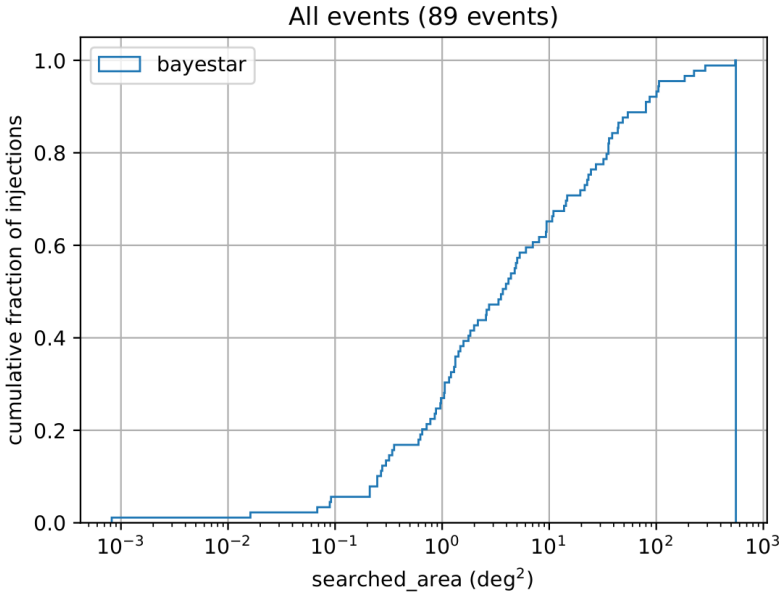

Figure 5: Fraction of events with searched area equal to or less than that particular searched area

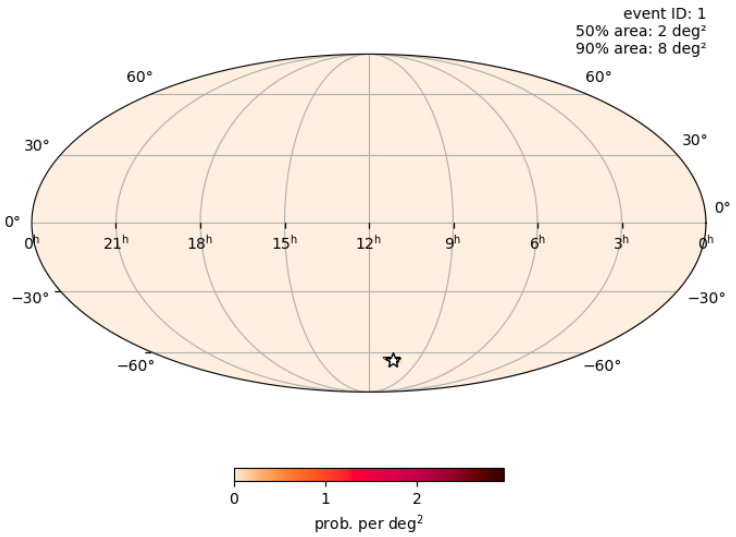

Figure 6: Mollweide Projection of a coincidence event

- Since the median searched area is 3.69 square degrees, 50% of sources are within the field of view of a single exposure of LSST.
- The Mollweide projection for an event localized by BAYESTAR is shown in Figure:6.
- For $d = 1161.14$ Mpc, the exposure time required is about 7 minutes for LSST.

4 Conclusion and Discussion

Results indicated that there is a plausibility that LIGO India's inclusion in the LIGO network can make NSBH merger detection with EM follow-up possible. It is yet to be determined how probable it is. The population distribution that is taken for this project is with no spin, but spin plays a role in determining whether or not an EM counterpart will be there or not. The model for the signal is taken as the one for the Binary Blackhole merger(BBH), so tidal disruption, which could lead to lower SNR, is not taken into account. Exposure time for LSST is calculated with simple arguments. In future work, the Focus will be on implementing all these changes for the calculation of the possibility of resolving the Hubble tension with NSBH mergers.

5 Acknowledgement

I would like to thank my supervisor, Prof. Sanjit Mitra, for his guidance and support throughout the project. I would also like to acknowledge Anirban Kopty and Kanchan Soni for their help. I also appreciate the fruitful discussions I had with Soumil.

References

[1] B. Schutz, *A first course in general relativity*. Cambridge University Press, 2009, pp. 189–194 and 203–210.

[2] L. Scientific and V. Collaborations, "The basic physics of the binary black hole merger GW150914," *Annalen der Physik*, vol. 529, no. 1-2, p. 1600209, Jan. 2017. [Online]. Available: https://onlinelibrary.wiley.com/doi/10.1002/andp.201600209

[3] S. Khan, S. Husa, M. Hannam, F. Ohme, M. Pürrer, X. J. Forteza, and A. Bohé, "Frequency-domain gravitational waves from nonprecessing black-hole binaries. II. A phenomenological model for the advanced detector era," *Physical Review D*, vol. 93, no. 4, Feb. 2016, publisher: American Physical Society (APS). [Online]. Available: https://link.aps.org/doi/10.1103/PhysRevD.93.044007

[4] M. Maggiore, *Gravitational Waves: Volume 1: Theory and Experiments*, 2007.

[5] J. Otis M. Solomon, "Psd computations using welch's method," Sandia National Laboratories,New Mexico, Tech. Rep., 1991.

[6] H.-Y. Chen, D. E. Holz, J. Miller, M. Evans, S. Vitale, and J. Creighton, "Distance measures in gravitational-wave astrophysics and cosmology," *Classical and Quantum Gravity*, vol. 38, no. 5, p. 055010, Jan. 2021, publisher: IOP Publishing. [Online]. Available: https://dx.doi.org/10.1088/1361-6382/abd594

[7] A. B. P. et al., "Prospects for Observing and Localizing Gravitational-Wave Transients with Advanced LIGO and Advanced Virgo," *Living Reviews in Relativity*, vol. 19, no. 1, Dec. 2016, publisher: Springer Science and Business Media LLC. [Online]. Available: http://link.springer.com/10.1007/lrr-2016-1

[8] S. Fairhurst, "Triangulation of gravitational wave sources with a network of detectors," *New Journal of Physics*, vol. 13, no. 6, p. 069602, Jun. 2011. [Online]. Available: https://iopscience.iop.org/article/10.1088/1367-2630/13/6/069602

[9] K. M. Górski, E. Hivon, A. J. Banday, B. D. Wandelt, F. K. Hansen, M. Reinecke, and M. Bartelmann, "HEALPix: A Framework for High-Resolution Discretization and Fast Analysis of Data Distributed on the Sphere," *The Astrophysical Journal*, vol. 622, no. 2, p. 759, Apr. 2005, publisher: IOP Publishing. [Online]. Available: https://iopscience.iop.org/article/10.1086/427976/meta

[10] L. P. Singer and L. R. Price, "Rapid Bayesian position reconstruction for gravitational-wave transients," *Physical Review D*, vol. 93, no. 2, p. 024013, Jan. 2016, arXiv:1508.03634 [gr-qc]. [Online]. Available: http://arxiv.org/abs/1508.03634

[11] E. Burns, "Neutron star mergers and how to study them," *Living Reviews in Relativity*, 2020.

[12] S. Vitale and C. Hsin-Yu, "Measuring the hubble constant with neutron star black hole mergers," *Physical Review Letters*, 2018.

[13] F. H. Shu, *The Physical Universe*, 1982.

[14] "Wikipedia article on roche limit." [Online]. Available: https://en.wikipedia.org/wiki/Roche_limit#cite_note-3

[15] "Wikipedia article on neutron star."

[16] L. P. Singer, L. R. Price, B. Farr, A. L. Urban, C. Pankow, S. Vitale, J. Veitch, W. M. Farr, C. Hanna, K. Cannon, T. Downes, P. Graff, C.-J. Haster, I. Mandel, T. Sidery, and A. Vecchio, "The First Two Years of Electromagnetic Follow-Up with Advanced LIGO and Virgo," *The Astrophysical Journal*, vol. 795, no. 2, p. 105, Oct. 2014, arXiv:1404.5623 [astro-ph]. [Online]. Available: http://arxiv.org/abs/1404.5623

[17] F. Foucart, M. Duez, L. Kidder, S. Nissanke, H. Pfeiffer, and M. Scheel, "Numerical simulations of neutron star-black hole binaries in the near-equal-mass regime," *Physical Review D*, vol. 99, no. 10, May 2019. [Online]. Available: http://dx.doi.org/10.1103/PhysRevD.99.103025

[18] N. Farrow, X.-J. Zhu, and E. Thrane, "The mass distribution of galactic double neutron stars," *The Astrophysical Journal*, vol. 876, no. 1, p. 18, Apr. 2019. [Online]. Available: http://dx.doi.org/10.3847/1538-4357/ab12e3

[19] K. A. Kuns, H. Yu, Y. Chen, and R. X. Adhikari, "Astrophysics and cosmology with a decihertz gravitational-wave detector: TianGO," *Physical Review D*, vol. 102, no. 4, p. 043001, Aug. 2020, arXiv:1908.06004 [gr-qc]. [Online]. Available: http://arxiv.org/abs/1908.06004

[20] P. Fagrelius, "Flat field calibration exposure time calculator." [Online]. Available: https://sitcomtn-049.lsst.io/

[21] R. L. Jones, "Calculating lsst limiting magnitudes and snr." [Online]. Available: https://smtn-002.lsst.io/